ELSEVIER

Journal of Molecular Catalysis A: Chemical 180 (2002) 109–123

JOURNAL OF MOLECULAR CATALYSIS A: CHEMICAL

www.elsevier.com/locate/molcata

# Synthesis of binaphthols over mesoporous molecular sieves☆

M. Ramakrishna Prasad, G. Kamalakar, S.J. Kulkarni*, K.V. Raghavan

*Indian Institute of Chemical Technology, Hyderabad 500 007, India*

Received 16 August 2000; received in revised form 8 November 2000; accepted 5 October 2001

## Abstract

Mesoporous aluminosilicates (Al-containing NaMCM-41) were applied as catalyst supports for oxidative coupling of β-naphthol and substituted β-naphthols due to their remarkable features such as surface area, ordered mesopores and high thermal stability. The NaMCM-41 supported copper catalysts prepared by impregnation method, and Cu-NaMCM-41 was prepared by incorporating copper during synthesis. Oxidative coupling of β-naphthol reaction was studied using molecular oxygen as oxidant. The copper supported NaMCM-41 catalysts were prepared with different Si/Al ratios and calcined from 120 to 420 °C were observed to show varied product selectivity. The NaMCM-41 supported copper catalysts and Cu-NaMCM-41 were more active than the corresponding Cu/Fe supported on NaY zeolite. The catalysts were characterized by X-ray diffraction (XRD), temperature programmed reduction (TPR), UV–DRS, ICPMS and BET surface area techniques and the reaction products were confirmed by $^1$H-NMR, FTIR and HRMS. An attempt has been made to explain the product selectivity of the catalysts discussed with the above techniques. The high dispersion of $Cu^{+2}$ species observed in the catalysts having high Si/Al ratios in NaMCM-41 support and catalysts that are calcined at low temperatures, i.e. less than 420 °C, yielded an unexpected product perylene diol. A comparatively low dispersion of $Cu^{+2}$ species, noticed in catalysts having low Si/Al ratios and calcined at high temperatures, yielded binapthol as the coupled product. The effect of the variation of catalyst and the solvent are also studied. © 2002 Elsevier Science B.V. All rights reserved.

*Keywords:* β-Naphthol; Oxidative coupling; $Cu_{imp}$NaMCM-41; Cu/$Fe_{imp}$NaY; Binaphthol; Perylene diol

## 1. Introduction

Mesoporous molecular sieves designated as M41S have attracted the attention of many researchers since their discovery at Mobil Oil Corporation [1,2,50]. These amorphous silica materials possess well-defined mesopores which consists of an array of unidimensional and hexagonally shaped mesopores, the diameters of which can be tailored to the desired value (18–100 Å) by the proper choice of surfactants, auxiliary organics, and synthesis parameters. Since the discovery of MCM-41, several reports have appeared on the isomorphous substitution of Si by other elements such as Ti [3,4], V [5,6], Sn [7,8], Cr [9], and Zr [10]. The isomorphous substitutions of these metal ions were active as catalysts for the selective oxidation of organic molecules under mild conditions. Copper supported silica catalysts are studied for the cyclohexanol dehydrogenation reactions [11–13]. Recently, copper modified MFI [14], FAU [15,16] and Mordenite [17,18] zeolites have been extensively studied for the selective catalytic reduction (SCR) of $NO_x$. Copper supported mesoporous silicates and aluminosilicates have been studied for the oxidation of benzene to phenol [19] and in the oxidation of 2,6-di-*tert*-butylphenol to 4,4$^1$-dihydroxy-3,3$^1$,

---

☆ IICT Communication No. 4552.

* Corresponding author.

*E-mail address:* sjkulkarni@iict.ap.nic.in (S.J. Kulkarni).

PII: S1381-1169(01)00412-5

$5,5^1$-tetra-*tert*-butyl-biphenyl ($H_2DPQ$) and $3,3^1$, $5,5^1$-tetra-*tert*-butyl-$4,4^1$-diphenoquinone (DPQ) [20] with molecular oxygen as oxidant under mild conditions. In the latter reaction, the conversion of 2,6-di-*tert*-butyl phenol was enhanced by adding alkali such as KOH, which facilitated the formation of phenolate anion.

Binaphthols and its analogs are widely used materials for the introduction of chirality in synthetic organic chemistry. Diels-Alder cycloadditions [21,22], Ene reactions [23,24], Lewis acid catalyzed transformations [25,26], and enantio-selective group transfer polymerizations [27,28] are few reactions which are catalyzed by binaphthol derivatives. The nature and high synthetic utility of binaphthols have created much interest in their synthesis. Efforts in the direction of preparation of binaphthols have lead to the use of $FeCl_3$ [29], $K_4Fe(CN)_6$ [30], $Mn(acac)_3$ [31], Cu(II)-amine complexes [32] in homogeneous media to oxidize β-naphthol to BINAPs. But these routes suffer from disadvantages like separation of the product from the reaction mixture, requirement of stoichiometric quantities of reagents, non-reusability of reagent. To avoid these problems, heterogeneous catalytic routes are adopted. In the present work, we have used copper supported mesoporous NaMCM-41 (with various Si/Al ratios) materials as catalysts for the oxidative coupling of β-naphthol and substituted β-naphthols. Copper supported mesoporous materials are prepared by impregnation method, the product selectivity in β-naphthol coupling reaction is varied depending upon the catalyst used for the reaction. One of the products of this reaction, a perylene derivative, has very good medicinal significance as it is used in the preparation of antiviral agents [33] such as shiraiachrome A and shiraiachrome B. The catalysts have been characterized by X-ray diffraction (XRD), temperature programmed reduction (TPR), UV–DRS and BET surface area to explain the product selectivity.

## 2. Experimental

### 2.1. Synthesis of NaMCM-41

NaMCM-41 materials with various Si/Al ratios were prepared in our laboratory by the procedure reported elsewhere [34]. The molar composition of the synthesis gel is (0.345–1.9) $Al_2O_3$:31.01 $SiO_2$:2.2 $(surfactant)_2O$:3.16 $(TEA)_2O$:1.89 $Na_2O$:615–802 $H_2O$. 0.76 g of aluminum isopropoxide, and 0.3 g of sodium hydroxide were taken in a 100 ml glass beaker, to which 20 ml of distilled water was added and stirred thoroughly under heating at 80 °C until a clear solution was obtained. The solution was cooled to room temperature followed by drop-wise addition of 9.26 g of 20 wt.% of aqueous tetraethylammonium hydroxide. The resultant mixture was stirred for 2 h. In a separate beaker, 9.26 g of Ludox silica (40 wt.% in water) was added to 30 ml of distilled water and stirred until a uniform mixture was obtained. To this solution, the sodium aluminate mixture was added drop-wise. The resultant mixture was stirred for 3 h and 10.55 g of cetyltrimethylammonium bromide (25 wt.% in water) was added in small quantities. After stirring for 1 h, the pH of the resulting gel was adjusted to 12 using dilute ammonia solution and transferred to an autoclave and heated at a temperature of 100 °C in static condition for 48 h in an oven. The autoclave was cooled and the solid material was filtered, and thoroughly washed with distilled water. The catalyst was dried and calcined at 500 °C overnight in the presence of static air to remove the surfactant.

### 2.2. Preparation of Cu-supported catalysts

Zeolite Y is obtained from the PQ Corpn., USA, NaMCM-41 (synthesized in our laboratory) were used as supports. Copper modified catalysts were prepared by wet impregnation technique. The support (NaMCM-41/NaY) in prescribed amounts were soaked in aqueous cupric nitrate (S. D. Fine Chem Ltd., Laboratory reagent grade) solution (5 wt.%) for 6 h and evaporated to remove the solvent, dried at 120 °C overnight and calcined at different temperatures in the static air flow. One set of copper ion supported NaMCM-41 catalysts 1a ($Si/Al = 16.5$), 2a ($Si/Al = 30$), 3a ($Si/Al = 60$) and 4a ($Si/Al = 90$) catalysts were dried at 150 °C and used as such in reactions and for TPR studies as shown in Fig. 4. Another set of catalysts were prepared by calcining $Cu_{imp}$NaMCM-41 ($Si/Al = 30$) at various temperatures, i.e. 2b, 2c and 2d at 200, 300 and 420 °C, respectively. Cu/$Fe_{imp}$NaY catalysts were calcined at 420 °C.

#### 2.2.1. Synthesis of copper Al-NaMCM-41 (incorporated in synthesis gel)

0.5 g of aluminum isopropoxide, and 0.4 g of sodium hydroxide were taken in a 100 ml glass beaker, to which 20 ml of distilled water was added and stirred thoroughly under heating at 80 °C until a clear solution was obtained. To this solution, 0.7 g of cupric nitrate dissolved in water was added under stirring. Then this solution was cooled to room temperature followed by drop-wise addition of 9.26 g of tetraethylammonium hydroxide (20 wt.% in water). The resultant mixture was stirred for 2 h. In a separate beaker, 9.26 g of Ludox silica (40 wt.% in water) was added to 30 ml of distilled water and stirred until a uniform mixture was obtained. To this solution, the copper dissolved in sodium aluminate mixture was added drop-wise. The resultant mixture was stirred for 3 h and 10.55 g of cetyltrimethylammonium bromide (25 wt.% in water) was added in small quantities. After stirring for 1 h, the pH of the resulting gel was adjusted to 12 using dilute ammonia solution and transferred to an autoclave and heated at a temperature of 100 °C for 48 h in an oven. The autoclave was cooled and the solid material was filtered and washed thoroughly with distilled water. The catalyst was dried and calcined at 500 °C overnight in the presence of static air to remove the surfactant.

### 2.3. X-ray diffraction

The XRD pattern of the materials used in this reaction were recorded on D 5000 Seimens X-ray diffractometer with Ni-filtered Cu K$\alpha$ radiation ($\lambda = 1.5406$ Å).

### 2.4. BET surface area

BET surface area was determined by $N_2$ physisorption on Autochem 2910 (Micromeritics, USA) using BET single point method.

### 2.5. Temperature programmed reduction

The temperature programmed reduction patterns were recorded on Autochem 2910 (Micromeretics instrument, USA). The unit has a programmable furnace with a maximum operating temperature of 1100 °C. The instrument was connected to a computer, which performs tasks such as programmable heating, cooling cycles, continuous data recording, gas valve switching, data storage and analysis. In a typical experiment for TPR, about 50 mg of oven-dried sample (dried at 100 °C for 16 h) was taken in a U-shaped quartz sample tube. The catalyst was packed between two plugs of quartz wool in one side of the quartz tube. The temperature was monitored with the aid of thermocouples located near the sample from outside and also on the top of the sample. Highly sensitive mass-flow controllers (Brooks, USA) were used for monitoring the gas flows. Prior to the TPR studies, the catalyst sample was pretreated by passing helium purified by molecular sieves (50 ml min$^{-1}$) at 200 °C for 2 h. The flow (50 ml min$^{-1}$) of reducing gas consists of 5% hydrogen and the balance argon which is purified by passing through oxy-trap and 4 Å molecular sieves is maintained through the catalyst. The temperature-programming rate is maintained at 10 °C min$^{-1}$ from 30 to 1000 °C. The water vapor produced during reduction of the catalyst was condensed with a cold trap, which consists of isopropanol saturated with liquid nitrogen. The hydrogen concentration in the effluent stream was monitored with the thermal conductivity detector and the areas under the peaks were integrated using GRAMS/32 software. $H_2$ calibration was performed by the reduction of known amount of high purity $Ag_2O$ to Ag, a method which was found to be more reliable and reproducible than by injecting known volumes of hydrogen pulses to the detector.

### 2.6. UV-diffuse reflectance spectra

The nature of copper species was determined by UV–visible spectroscopy. Diffuse reflectance spectra were recorded in the UV-region (200–900 nm) at a split width of 1.5 nm and scan speed of 400 nm per minute with GBC Cintra 10e UV visible spectrometer for the catalyst samples. Pellets were made by taking ~15 mg of catalyst sample and dried KBr, grinded thoroughly for uniform mixing before making pellet, the spectrum was recorded at room temperature.

### 2.7. Liquid phase oxidation of β-naphthol

In a typical reaction of oxidative coupling of β-naphthol, substrate along with the catalyst and solvent (all the details of the catalyst and substrate are given in corresponding tables) are taken in 50 ml three necked round bottomed flask and are stirred in the presence of air bubbling. The progress of the reaction was monitored by thin layer chromatography (TLC). After the completion of the reaction, the solvent is vacuum evaporated and products were isolated using column chromatography. The products of the reaction were confirmed by $^1$H-NMR, FTIR and HRMS.

## 3. Results and discussion

The XRD patterns of the NaMCM-41 with various Si/Al ratios of 16.5, 30, 60 and 90 are presented in Fig. 1. The intense low angle $2\theta$ peak and peaks between 3 and 5° indicate the formation of the mesoporous materials [35]. The sharp peak ascribed to the (1 0 0) reflection of the hexagonal structure of

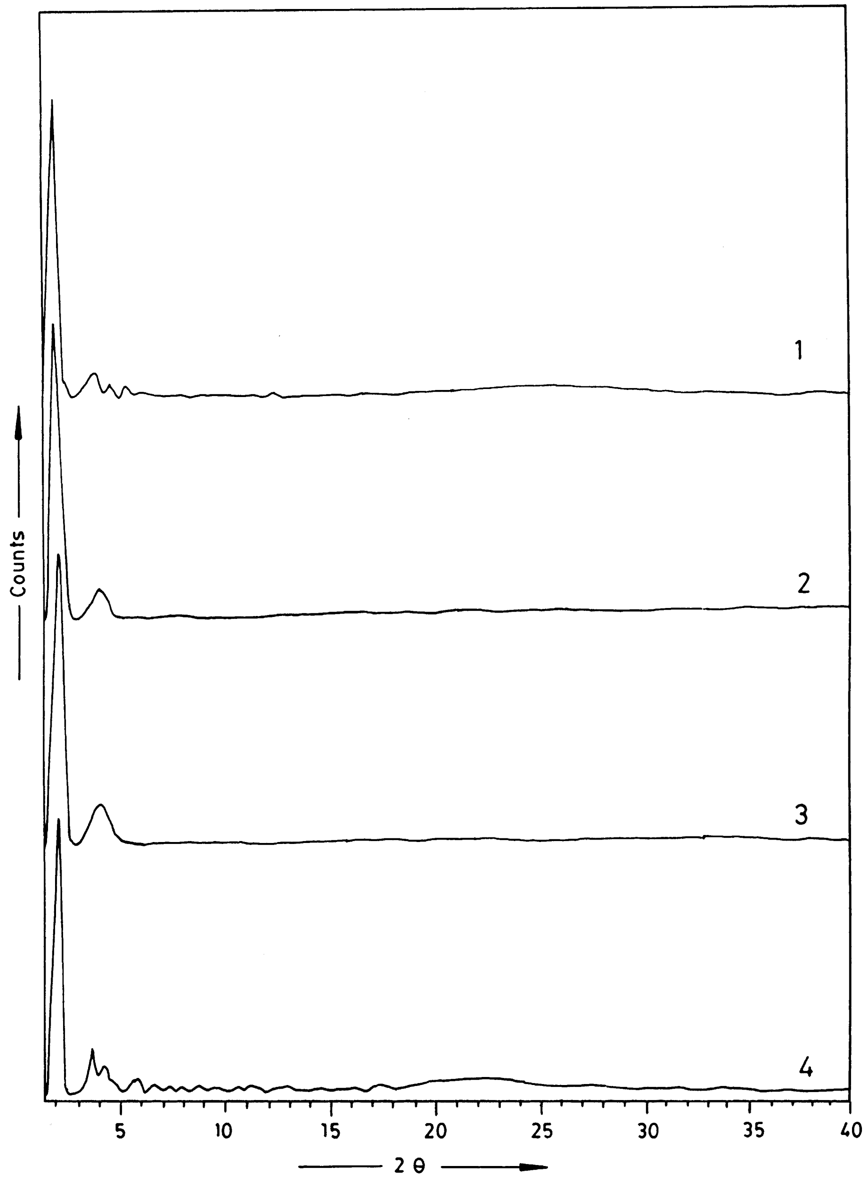

Fig. 1. XRD patterns of calcined NaMCM-41 with Si/Al ratios: (1) 16.5; (2) 30; (3) 60; (4) 90.

the mesopores was observed at $2\theta = 2.0$–$2.2^\circ$ corresponding to $d = 4.1$–$4.4$ nm. Besides the strong peak, weak peaks were ascribed to (1 1 0) and (2 0 0) reflections observed at $2\theta = 3$–$5^\circ$, $d = 2.1$ and 2.3 nm, respectively. The peaks indicated that the long-range order structure of mesoporous aluminosilicate catalysts. These peaks were broadened and shifted slightly to higher angle with increasing aluminum content. These results showed that the regularity of the mesoporous structure decreased and the pore size became slightly narrower with the decrease in Si/Al ratio. XRD patterns of $\mathrm{Cu_{imp}}$NaMCM-41 catalysts dried at 120 °C showed copper nitrate hydroxide ($Cu_2(OH)_3NO_3$, ASTM file No. 15-14) in $\mathrm{Cu_{imp}}$NaMCM-41 (Si/Al = 90) with more intensity and it decreases in remaining catalysts with the decrease of the Si/Al ratio of the NaMCM-41 support (Fig. 2). Since hydrated copper nitrate species are present in the framework of NaMCM-41, sharp $d_{100}$ peak intensity decreased as shown in Fig. 2. There is no copper species observed in the X-ray patterns of $\mathrm{Cu_{imp}}$NaMCM-41 catalysts dried or calcined at above 200 °C (Fig. 3). After the modification of NaMCM-41 catalysts with copper, the $d_{100}$ values (Table 1) of $\mathrm{Cu_{imp}}$NaMCM-41 decreased than the parent NaMCM-41 supports. The cupric nitrate hydrate type of moieties that reacted with Si–OH groups of mesoporous surface decreased the pore size of the hexagonal channels in $\mathrm{Cu_{imp}}$NaMCM-41 catalysts dried at 120 °C.

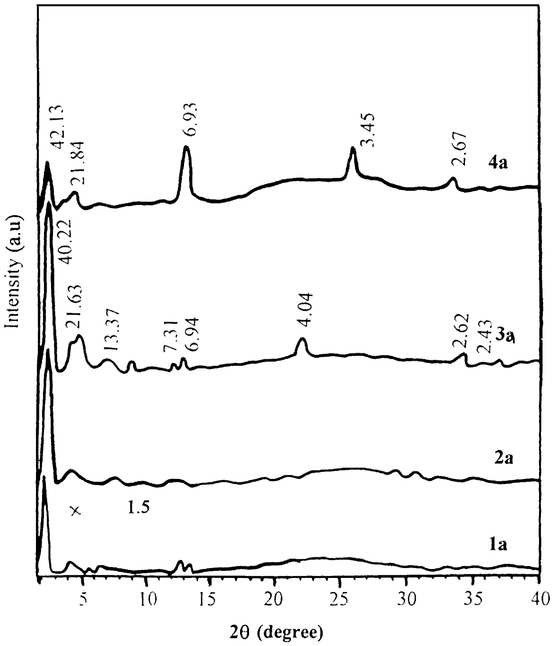

Fig. 2. XRD patterns of $\mathrm{Cu_{imp}}$NaMCM-41 with Si/Al ratios: (1a) 16.5; (2a) 30; (3a) 60; (4a) 90 dried at 120 °C.

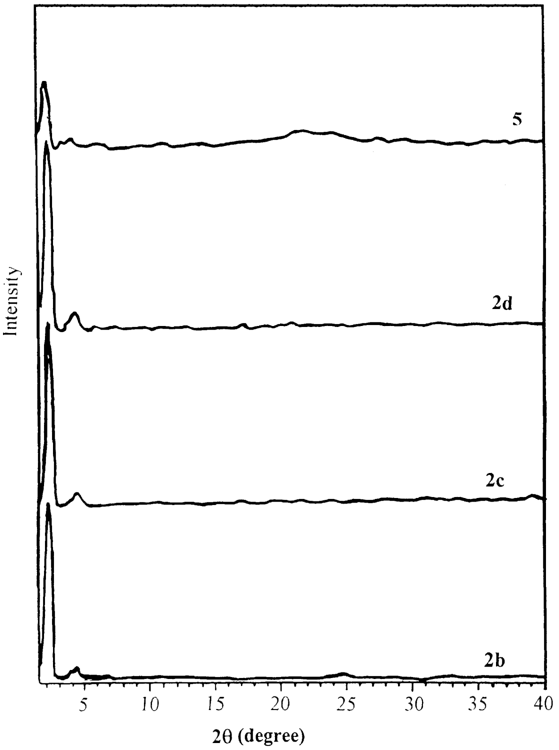

Fig. 3. XRD patterns of $\mathrm{Cu_{imp}}$NaMCM-41 (Si/Al = 30) calcined at various temperatures: (2b) 200 °C; (2c) 300 °C; (2d) 420 °C; (5) Cu-NaMCM-41 (copper incorporated in the synthesis) calcined at 500 °C.

The TPR profiles depicted in Fig. 4 have shown two distinctive peaks after deconvolution indicating that the reduction of $Cu^{+2}$ can be either consecutive process via $Cu^{+}$ to $Cu^{0}$ [36] or $Cu^{+2}$ is directly reduced to $Cu^{0}$ [15,16]. Other possibility is the presence of two different $Cu^{+2}$ species. The latter one is more probable, since the intensities of the two peaks are not the same. Therefore, one can visualize that $Cu^{+2}$ ions impregnated are undergoing reduction differently. In copper and nickel exchanged faujasite zeolites [15,16,37], two peaks were observed in low temperature region (177–577 °C) including one peak in high

Table 1
Physico-chemical properties of Cu-MCM-41 catalysts[a]

| S. No. | Catalyst | $d_{100}$ value | BET surface area (m$^2$ g$^{-1}$) | $H_2$ consumed (μmoles g$^{-1}$) |
|---|---|---|---|---|
| 1 | NaMCM-41 (16.5) | 44.25 | 871 | – |
| 1a | Cu$_{imp}$NaMCM-41 (16.5) | 43.99 | 846 | 166 |
| 2 | NaMCM-41 (30) | 41.92 | 898.7 | – |
| 2a | Cu$_{imp}$NaMCM-41 (30) | 41.95 | 776 | 531 |
| 3 | NaMCM-41 (60) | 41.83 | 955 | – |
| 3a | NaCu$_{imp}$MCM-41 (60) | 40.22 | 882 | 894 |
| 4 | NaMCM-41 (90) | 43.11 | 1020 | – |
| 4a | Cu$_{imp}$NaMCM-41 (90) | 42.13 | 428 | 1074 |
| 5 | Cu-NaMCM-41 | 43.68 | 610 | 295 |
| 2b | Cu$_{imp}$NaMCM-41 (30) | 41.99 | – | 620 |
| 2c | Cu$_{imp}$NaMCM-41 (30) | 41.38 | – | 416 |
| 2d | Cu$_{imp}$NaMCM-41 (30) | 41.22 | – | 201 |
|  |  |  |  | 282 |

[a] Entries 1a–4a: after modification of the catalysts with copper, dried at 120 °C. In entries 1a–4a and 2b–2d, Si/Al ratios in the parenthesis are from initial gel, entry 5: Cu-NaMCM-41, copper incorporated during the synthesis. Entries 2a, 2b and 2c are dried/calcined at 200, 300 and 420 °C, respectively.

temperature region. Two peaks in the low temperature region were attributed to Cu$^{+2}$ present in super cages and sodalite cages or in hexagonal prisms of FAU zeolites, i.e. Cu$^{+2}$ to Cu$^{0}$ reduction step. The high temperature peak (>727 °C) is assigned to Cu$^{+}$ to Cu$^{0}$ reduction. In mesoporous M41s having unidimensional hexagonal uniform channels, there is no possibility of forming two types of Cu$^{+2}$ ions like in copper ions in super and sodalite cages. The copper impregnated Faujasite [15] Cu (196) FAU showed only one peak in low temperature region. In the present TPR profiles of all the copper impregnated MCM-41 catalysts have not shown any high temperature peaks, which is supporting the absence of Cu$^{+1}$ species (TPR was studied up to 1000 °C). In Cu$_{imp}$NaMCM-41 catalysts, having different Si/Al ratios have shown two peaks as depicted in Fig. 4 in the range of 230–350 °C and the hydrogen consumption is increased from $Si/Al = 16.5$ to 90. The reduction profiles (Fig. 4) show the presence of the Cu$^{+2}$ species over NaMCM-41 support in two distinct environments, viz. the interaction between the metal ions and the support, and the presence of bulk Cu$^{+2}$ species. Hydrogen consumption values from TPR gave a clear picture of the dispersion of copper (interacted Cu$^{+2}$ species; $T_{max} = 230\,°C$) on different NaMCM-41 supports. As there is an increase in the Si/Al ratio of the NaMCM-41 support, there is a gradual increase in the copper dispersion as seen in Fig. 4. The decrease in the surface area of NaMCM-41 catalysts (Table 1) after modification with copper may be due to the presence of bulk Cu$^{+2}$ species. The drastic decrease of surface area in Cu$_{imp}$NaMCM-41 ($Si/Al = 90$) with high Si content is due to the presence of Cu$^{+2}$ species and Cu$^{+2}$ interacted species. The increase in the intensity of bulk Cu$^{+2}$ species along with the interacted Cu$^{+2}$ species can be observed from TPR pattern (Fig. 4). XRD results also confirmed the presence of larger Cu$^{+2}$ species (in the form of $Cu_2(OH)_3NO_3$) and the $d_{100}$ signal with low intensity. Increase in Si/Al ratio of NaMCM-41 support will decrease the acidic strength [38,39] which in turn will increase the dispersion of copper. From earlier studies [38–40], it is known that the M41S having high silica possesses more surface area, this is also one of the possible reasons for the high dispersion of copper for Cu$_{imp}$NaMCM-41 ($Si/Al = 90$). The Cu$_{imp}$NaMCM-41 ($Si/Al = 90$), 60, 30, 16.5 dried at 120 °C have shown first reduction peak at 238, 273, 290, and 230.76 °C and the second peak at 278, 319, 353 and 255.0 °C, respectively. Copper on silica prepared by the ion exchange method [41] showed only one reduction peak at 232 °C which was assigned to finely dispersed copper having a size around 1.4 nm. The strongest peak observed at 277–317 °C for silica supported copper catalysts prepared by deposition–precipitation method

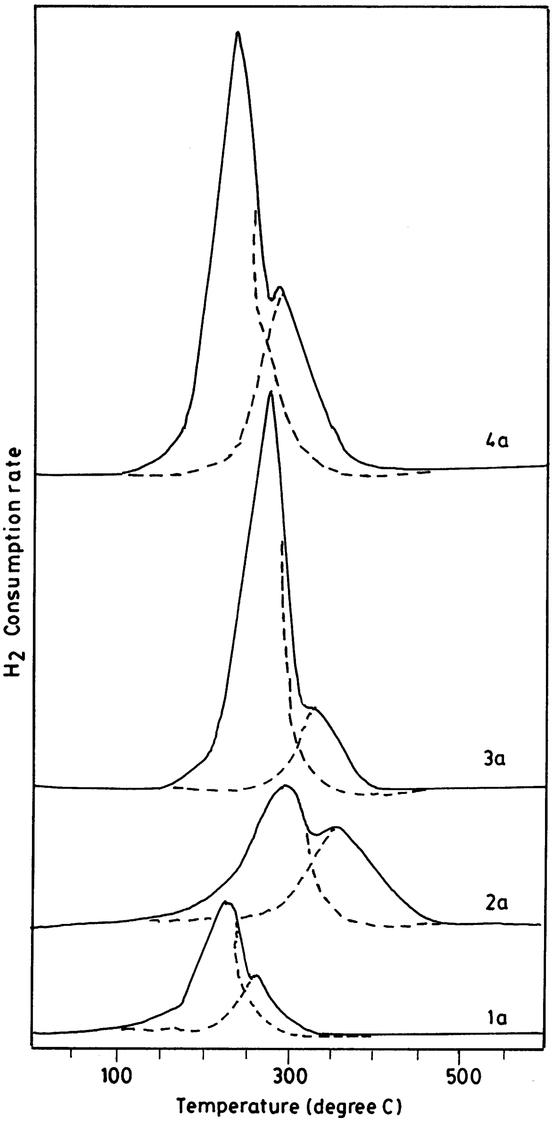

Fig. 4. TPR profiles of $Cu_{imp}$NaMCM-41 with Si/Al ratios: (1a) 16.5; (2a) 30; (3a) 60; (4a) 90 dried at 120 °C.

at various temperatures 20, 60 and 90 °C is assigned to larger copper particles having physical properties similar to that of bulk copper phase [12]. According to assignment done by others, the first and second reduction peaks in the copper impregnated NaMCM-41 catalysts can be attributed to two types of copper particles. The former can be assigned to finely dispersed copper particles having small particle sizes and the latter to large copper particles having physical properties similar to that of bulk copper. TPR profiles for CuNaMCM-41 (Si/Al = 30) catalysts calcined or dried at various temperatures are depicted in Fig. 5. The effect of calcination on the dispersion of metal species in a catalyst earlier studied by van Hardeveld

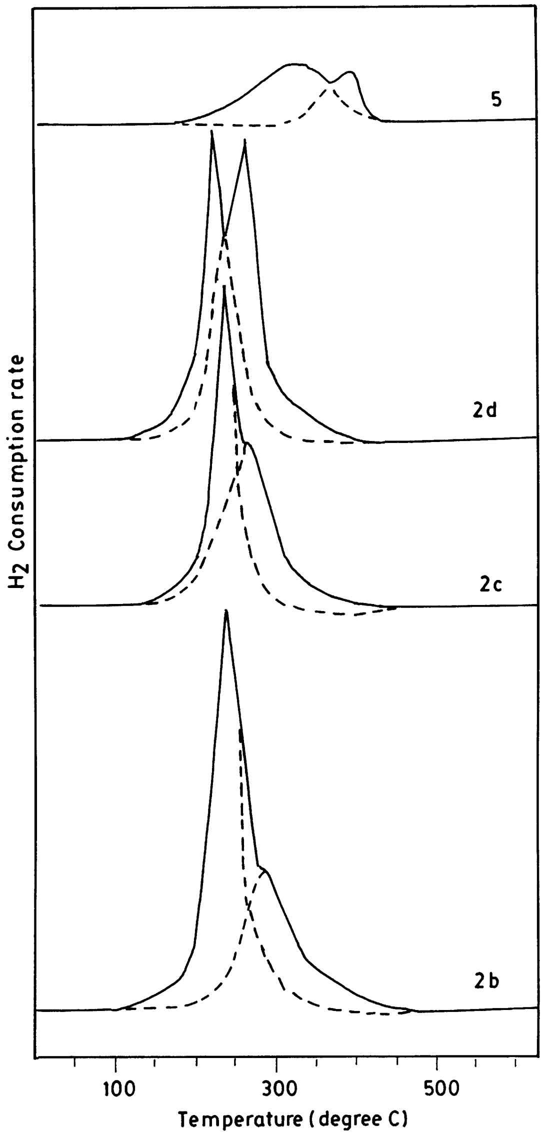

Fig. 5. TPR profiles of $Cu_{imp}$NaMCM-41 (Si/Al = 30) calcined at various temperatures: (2b) 200 °C; (2c) 300 °C; (2d) 420 °C; (5) Cu–NaMCM-41 (copper incorporated during the synthesis) calcined at 500 °C.

and van Montfoort [43]).[1] In nickel supported over silica catalysts prepared using nickel nitrate solution, direct reduction of dried catalyst resulted in high dispersion of nickel over silica support when compared to the calcined nickel supported silica catalysts. This was assigned to the sintering of nickel species, which led to the formation of larger particles. From our TPR study for $Cu_{imp}$NaMCM-41 ($Si/Al = 30$) calcined at different temperatures the following observations were made: (1) with increase in the calcination temperature, hydrogen consumption decreased, which is similar to the previous reports [11]; (2) with increase in calcination temperature of catalyst, the shoulder-like second reduction peak in dried samples is enhanced and simultaneously separated from the first reduction peak. The increase in the second reduction peak is due to the agglomeration and/or sintering of copper particles, i.e. finely dispersed small particles are converting into larger copper particles. The finely dispersed copper oxide particles over NaMCM-41 reduced more easily than bulk oxide, probably due to the high dispersion, which is reported in the literature.[1] In the TPR pattern of Cu-NaMCM-41 (copper incorporated during synthesis) calcined at 500 °C, the reduction peaks are shifted to higher temperatures as shown in Fig. 5. In this catalyst, the copper particles formed are larger and similar to bulk copper oxide. In Table 1, from hydrogen consumption values, it is observed that the copper dispersion is high for dried catalysts at 120 °C compared to the catalysts calcined at high temperatures. From these results, it can be concluded that the dispersion of the copper species (interacted $Cu^{+2}$ species) in the catalyst prepared by impregnation with copper nitrate strongly depends on the thermal pretreatment prior to the reduction. The observation was made by others for copper supported silica catalyst [11]. For the $Cu_{imp}$NaMCM-41 catalysts which are dried at 120 °C, the hydrogen consumption exceeds the amount of hydrogen needed for reduction of the copper(II) to zero valent copper, the thermal pretreatment of catalyst which affects the total hydrogen consumption due to reduction of (copper) nitrate present in this precursor. Direct reduction of the copper nitrate in the dried catalysts at 120 °C may give rise to retention of nitrogen atoms in the reduced copper catalyst [11,44]. The hydrogen consumption for $Cu_{imp}$NaMCM-41 ($Si/Al = 30$) catalyst calcined at 420 °C also exceeds the required amount to reduce $Cu^{+2}$ ions. It is reported for copper supported silica catalysts prepared by co-precipitation method [11] calcined at 427 °C that the total hydrogen consumption exceeds the amount of hydrogen needed for complete reduction of the metal in the catalyst. The Cu-NaMCM-41 (copper incorporated during synthesis) calcined at 500 °C showed $H_2/Cu$ ratio to be approximately 1 which gave an evidence that this catalyst possesses $Cu^{+2}$ ions in the framework. For the present, $Cu_{imp}$NaMCM-41 catalysts contain various kinds of copper particles: finely dispersed copper, larger particles of bulk copper phase and mixtures of the two.

Fig. 6 illustrates the DR spectra of the $Cu_{imp}$-NaMCM-41 catalysts having different Si/Al ratios of NaMCM-41 support. Three main peaks in the spectra were observed at 220–293, 335–483 and 527–767 nm regions. The region between 527–767 nm band can be attributed to the d–d transition of Cu with octahedral environment in CuO as proposed in the case of Cu impregnated over FAU zeolites [14], zirconia [45], and alumina [46] supported CuO. The second band observed in Fig. 6 shows very much similarity with the pure CuO obtained by calcining cupric nitrate spectra shown bands at 325–475 and 475–750 nm (Fig. 7). So the second band can be ascribed to charge transfer bands between mononuclear $Cu^{+2}$ and oxygen ($Cu^{2+} \rightarrow O$) and/or cluster $Cu^{+2}$ and oxygen (e.g. $(Cu–O–Cu)^{+2}$ species). Among the three peaks, the first peak is predominant in all the DR spectra of the catalysts prepared by impregnation method. Pure NaMCM-41 support shows a peak at 215–315 nm, so the first peak region can be assigned to the support. But while comparing the DR spectra of pure cupric nitrate, a peak at 210–340 nm was observed, which is giving an evidence that the first peak may be even due to cupric nitrate present in the above modified samples, because these set of catalysts are not calcined and only dried at 120 °C. Komatsu et al. [14] ascribed charge transfer transitions occurring at 225 nm to $O \rightarrow Cu^{2+}$ in copper modified FAU zeolites. Schoonheydt [47] attributed this band to the copper $^2E_g \rightarrow {}^2T_{2g}$ transition, whereas in copper supported on silica catalysts prepared by impregnation method, the peaks around 250–400 nm have been identified

---

[1] See comment of R. van Hardeveld, in discussion of R.P. Eischens and J. Jacknow [42].

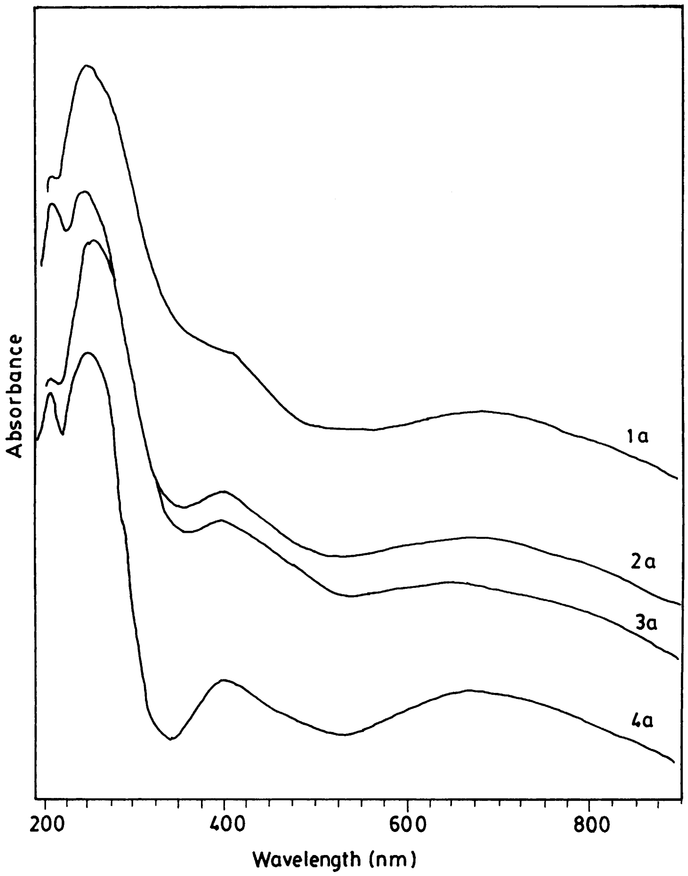

Fig. 6. Diffuse reflectance spectra of $Cu_{imp}$NaMCM-41 with Si/Al ratios: (1a) 16.5; (2a) 30; (3a) 60; (4a) 90 dried at 120 °C.

as the charge transfer bands between mononuclear $Cu^{+2}$ and oxygen (e.g. $(Cu–O–Cu)^{+2}$). In the present study, from Figs. 6 and 7, there should be two types of $Cu^{+2}$ isolated sites present in the copper supported NaMCM-41 catalysts. By calcining samples at higher temperature, the second peak region at 335–483 nm region is gradually increasing, as shown in Fig. 8. In one way, it can be ascribed to increase in the calcination temperature, the finely dispersed copper particles are forming clusters of copper as explained in case of TPR studies. Marison et al. [48] reported that the DR peak at around 620 nm is due to the bulk copper oxide (CuO) is observed in all DR spectra of the present samples. Since the 5 wt.% copper used for impregnation over NaMCM-41 catalysts which is very low, hence very low levels of bulk oxide was shown in the UV–DRS spectra of all the samples (Figs. 6 and 7). The peak at 700–900 nm has been attributed [13,49] to d–d transition band of a $Cu^{+2}$ ion centered in a pseudo-octahedral environment. All DR spectra of the samples showed bulk copper oxide and $Cu^{+2}$ ion centered in a pseudo-octahedral environment (Table 2).

Oxidative coupling of β-naphthol (Fig. 9) and substituted β-naphthols was carried out over $Cu_{mp}$Na-MCM-4 (Si/Al = 30) calcined at 420 °C which gave complete conversion of starting materials (Table 3). Oxidative coupling of β-naphthol was carried out over $Cu_{imp}$NaMCM-41 catalysts having different Si/Al ratios, which are dried at 120 °C (Table 4). The copper modified NaMCM-41 support having high Si/Al ratio yielded perylene diol and formation of former decreased in the catalysts having low Si/Al ratio NaMCM-41 supports (Table 4). Binaphthol was formed in the catalysts having NaMCM-41 support

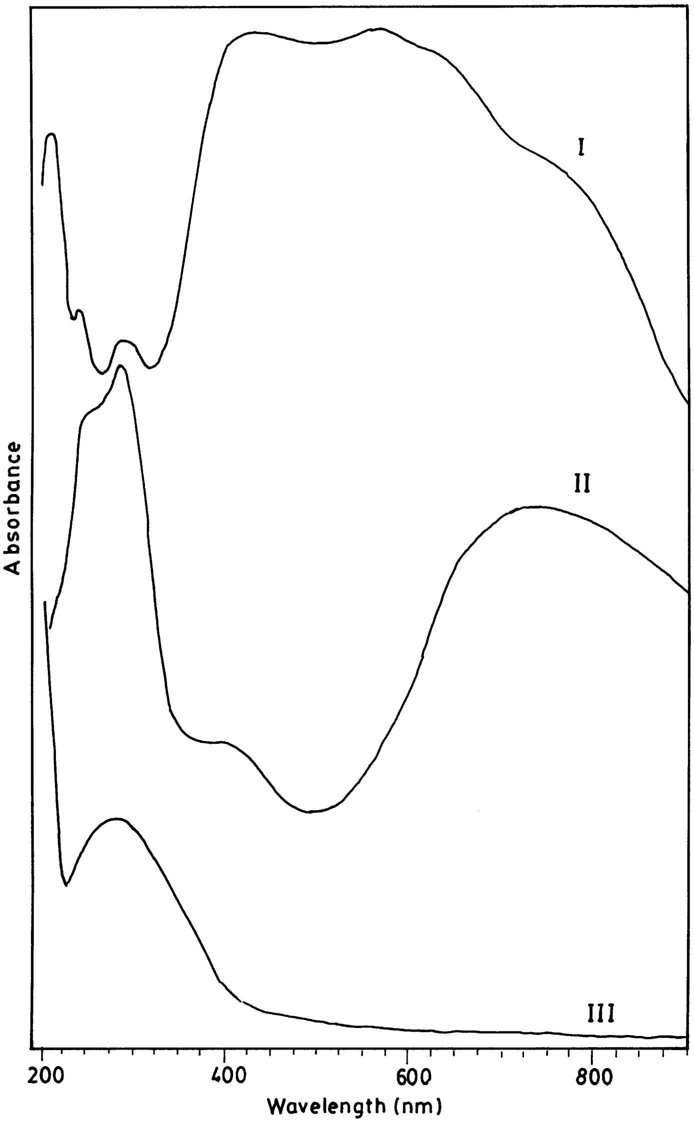

Fig. 7. Diffuse reflectance spectra of: (I) copper oxide (obtained by calcining $Cu(NO_3)_2$ at 400 °C); (II) cupric nitrate; (III) pure NaMCM-41 support.

with low Si/Al ratio and gradual decrease was observed with increase in Si/Al ratio of NaMCM-41 support. By increasing Si/Al ratio of the basic support NaMCM-41, the hydrogen volume consumed is increasing giving an evidence that the samples having sufficient quantity of finely dispersed $Cu^{+2}$ will be reduced to $Cu^0$ either by single step or by two steps which showed the higher selectivity for perylene diol. From TPR studies, it is observed that $Cu_{imp}$NaMCM-41 (Si/Al = 90) and (60) catalysts consumed more hydrogen to reduce $Cu^{+2}$ to $Cu^0$ when compared to the other two catalysts which has low Si/Al ratios. From the catalytic activity studies, the exception is the $Cu_{imp}$NaMCM-41 (90), and $Cu_{imp}$NaMCM-41 (60) catalysts which were calcined below 400 °C to obtain perylene type of product.

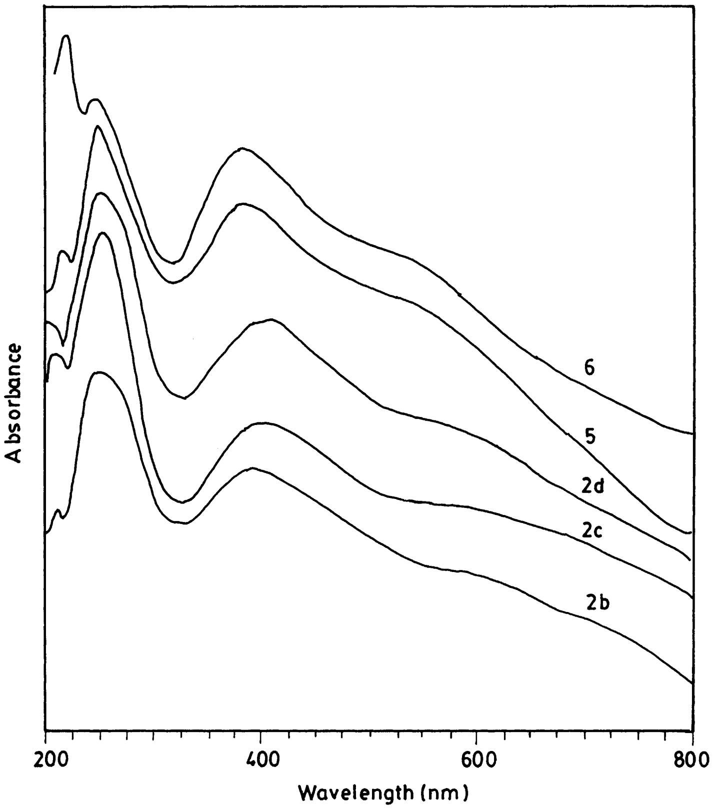

Fig. 8. Diffuse reflectance spectra of $Cu_{imp}$NaMCM-41 (Si/Al = 30) calcined at various temperatures: (2b) 200 °C; (2c) 300 °C; (2d) 420 °C; (5) Cu–NaMCM-41 (copper incorporated during in the synthesis) calcined at 500 °C; (6) $Cu_{imp}$NaMCM-41 (Si/Al = 90) after reaction.

This may be due to the fact that these, having enough amount of finely dispersed copper particles, cause the formation of perylene diol. Upon calcination of these catalysts at above 400 °C, the copper particles which increased in size are inactive for the formation of perylene diol, instead they are active for the formation of binaphthol. This can be assigned from the TPR patterns of the $Cu_{imp}$NaMCM-41 (Si/Al = 30) calcined at various temperatures, where the second reduction peak is increasing in the catalysts, which are calcined at high temperatures. Here high surface area and mild acidity of NaMCM-41 (Si/Al = 90) are favored for high copper dispersion which in turn yielded perylene diol. Simple bulk copper oxide

Table 2
Elemental analysis of the samples[a]

| S. No. | Catalyst | Al (wt.%) | Na (wt.%) | Cu (wt.%) | Na/Al (mol/mol) | Cu/Al (mol/mol) |
|---|---|---|---|---|---|---|
| 1 | $Cu_{imp}$NaMCM-41 (16) | 3.67 | 7.72 | 1.1 | 2.46 | 0.127 |
| 2 | $Cu_{imp}$NaMCM-41 (30) | 1.5 | 3.76 | 1.4 | 2.94 | 0.396 |
| 3 | $Cu_{imp}$NaMCM-41 (60) | 0.85 | 3.5 | 1.6 | 4.83 | 0.796 |
| 4 | $Cu_{imp}$NaMCM-41 (90) | 0.6 | 3.67 | 1.8 | 7.19 | 1.274 |
| 5 | Cu-NaMCM-41 | 1.44 | 1.5 | 1.1 | 1.22 | 0.324 |

[a] Entries 1–4: after modification with copper, catalysts are dried at 120 °C; entry 5: Cu–NaMCM-41, copper incorporated during the synthesis. In entries 1–4, the values in the parenthesis are Si/Al ratios from the synthesis gel. Elemental analyses performed using ICPMS.

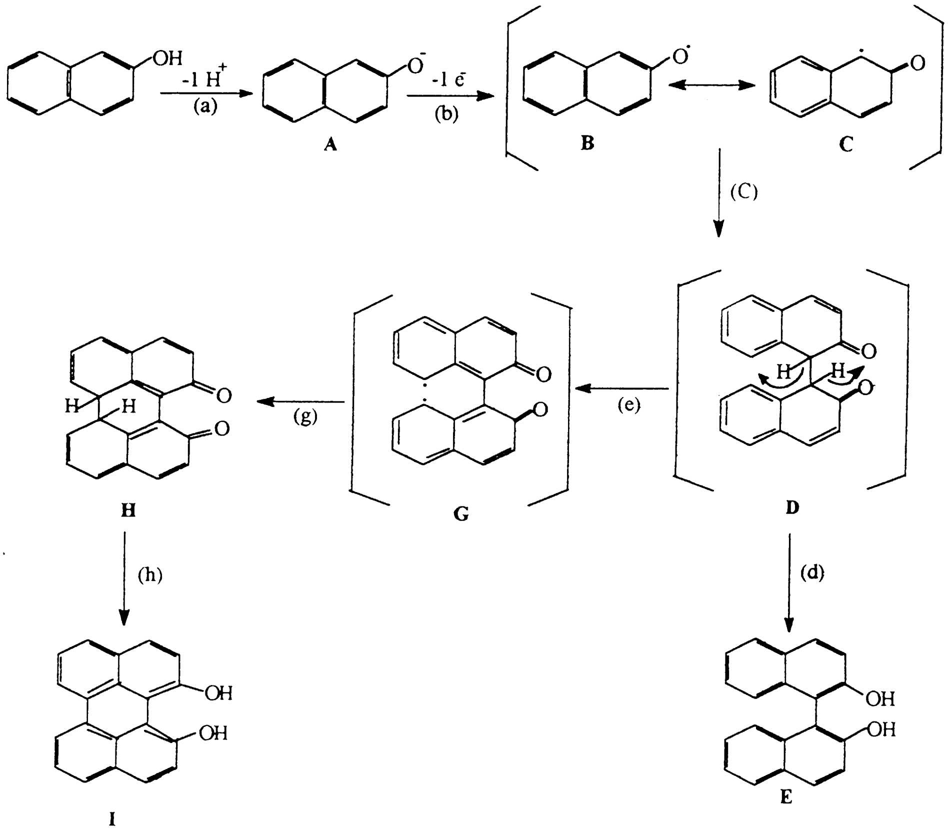

Fig. 9. Possible mechanism for oxidative coupling of β-naphthol.

Table 3
β-Naphthol coupling variation of substrate[a]

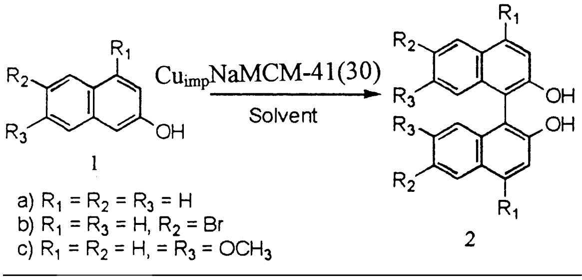

a) $R_1 = R_2 = R_3 = H$
b) $R_1 = R_3 = H$, $R_2 = Br$
c) $R_1 = R_2 = H$, $= R_3 = OCH_3$

| S. No | Starting material | Time (h) | Binapthols | Isolated Yield (%) |
|---|---|---|---|---|
| (1) | 1a | 6 | 2a | 95.0 |
| (2) | 1b | 2 | 2b | 90.0<br>85.0[II] |
| (3) | 1c | 6 | 2c | 93.0<br>80.0[II] |
| (4) | 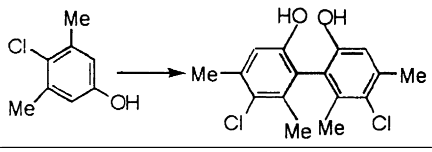 | 6 | – | 37.0 |

[a] Starting material: 280 mg, catalyst: 740 mg, IInd run with the catalyst. Reaction temperature: 135 °C; solvent: chlorobenzene (20 ml).

Table 4
β-Naphthol coupling with $Cu^{+2}{}_{im}$NaMCM-41 with various Si/Al ratios[a]

| S. No. | Catalyst | Conversion of β-naphthol (%) | Yield of the product (%) | Reaction time (h) |
|---|---|---|---|---|
| 1a | (1.1 wt.% $Cu^{+2}$) NaMCM-41 (16) | 100 | 97 (E) | 4.5 |
| 2a | (1.4 wt.% $Cu^{+2}$) NaMCM-41 (30) | 100 | 98 (E) | 5 |
| 3a | (1.6 wt.% $Cu^{+2}$) NaMCM-41 (60) | 100 | 40 (E) + 50 (I) | 6 |
| 4a | (1.8 wt.% $Cu^{+2}$) NaMCM-41 (90) | 100 | 95 (I) | 6 |
| 5 | (1.1 wt.% $Cu^{+2}$) NaMCM-41 | 100 | 93 (E) | 5 |
| 6 | Copper oxide | – | – | |

[a] Entries 1a–4a: catalysts prepared by impregnation method, dried at 120 °C; entry 5: copper incorporated during the synthesis; β-naphthol (280 mg), catalyst (740 mg). Solvent: chlorobenzene (20 ml), reaction temperature: 135 °C, E: binaphthol; I: perylene diol (structures of E and I are given in reaction mechanism).

Table 5
β-Naphthol coupling: variation of catalyst[a]

| S. No. | Catalyst | Conversion of β-naphthol (%) | Yield of binaphthol (E) (%) |
|---|---|---|---|
| 1 | $Cu_{imp}$NaMCM-41 (30) | 100 | 95 |
| 2 | $Fe_{imp}$NaMCM-41 (30) | 96 | 92 |
| 3 | $Cu_{imp}$NaY | 38 | 32 |
| 4 | $Fe_{imp}$NaY | 32 | 30 |

[a] Entries 1–4: catalysts are calcined at 420 °C, β-naphthol (280 mg), catalyst (740 mg). Solvent: chlorobenzene (20 ml); reaction temperature: 135 °C, reaction time: 6 h.

(prepared by calcination of cupric nitrate at 420 °C) was found to be inactive for the oxidative coupling reaction. From the above observation, it is clear that bulk copper oxide, which was formed at higher temperatures and at higher loading in $Cu_{imp}$NaMCM-41 catalysts, is inactive for this reaction, instead the interactive $Cu^{+2}$ ions with support are active for the oxidative coupling reaction.

The mechanism of oxidative coupling reaction of naphthol can be explained as follows. First deprotonation of naphthol will occur, which yields anion (A). The corresponding radical (B, C) is formed via one-electron transfer from the anion (A) to Cu (II) ion. There is another oxidation also possible in which one-electron loss from naphthol to form corresponding cation radical was followed by deprotonation leading to radical. The corresponding dimer is formed through C–C coupling of the two radicals (C). The dimer (D) easily rearranges to the more stable form, binaphthol (E). The product ‘H’ is generated by two consecutive deprotonation from ‘D’ which generates two free radicals in the dimer itself which results in

Table 6
β-Naphthol coupling: variation of solvent[a]

| S. No | Solvent | Reaction temperature (°C) | Conversion (%) | Yield of binaphthol (E) (%) |
|---|---|---|---|---|
| 1 | Chlorobenzene | 135 | 100 | 95 |
| 2 | Dichloromethane | 60 | 49 | 46 |
| 3 | 1,4-Dioxane | 107 | 30 | 28 |
| 4 | Methanol | 60 | – | – |

[a] Substrate: β-naphthol (280 mg), catalyst: $Cu_{imp}$NaMCM-41 (Si/Al = 30) (740 mg, calcined at 420 °C), solvent: 20 ml, reaction time: 6 h.

double coupling product, later it easily rearranges to stable tautomer, i.e. perylene diol (I).

Oxidative coupling of β-naphthol, was also carried out over $Cu_{imp}$NaMCM-41, $Fe_{imp}$NaMCM-41, $Cu_{imp}$NaY and $Fe_{imp}$NaY and the results are presented in Table 5. $Cu^{+2}$NaMCM-41 (30) gave complete conversion of starting material β-naphthol whereas this is not observed in the case of more acidic Cu/$Fe_{imp}$NaY materials. Low conversion of β-naphthol is observed in the case of modified NaY zeolites, which may be due to the difficulty in the diffusion of the coupled product of the smaller pore aperture of Y zeolite. The isolated coupled product yield was in the range 80–95%. The effect of the variation of solvent for this reaction is studied and the results are presented in Table 6. Chlorobenzene as solvent gave complete conversion of the β-naphthol whereas methanol did not show any conversion.

In conclusion, we found that $Cu_{imp}$NaMCM-41 catalyst was active for oxidative coupling for naphthol and substituted naphthols. The TPR provided a rapid fingerprint for the dispersion of copper species to explain the product selectivity. The NaMCM-41 support with sufficient and finely dispersed $Cu^{+2}$ particles was able to form perylene diol and the other catalysts do not have enough finely dispersed $Cu^{+2}$ particles which formed binaphthol. We also found the influence of pretreatment temperature and how it influences the product selectivity. It is observed from the conversion of finely dispersed copper species to larger copper species by increasing the calcination temperature. UV–DRS found supportive technique to explain the two types of copper species which showed two types of $Cu^{+2}$ peaks in the spectra. Enhancement of second peak that is observed at high calcination temperatures in the same way was explained in TPR studies for $Cu_{imp}$NaMCM-41 catalysts.

## Acknowledgements

We thank Dr. K.V.R. Chary, and Dr. K.S. Rama Rao for TPR study and helpful discussions. MRKP and GK thanks CSIR, New Delhi, for the financial assistance. We are also thankful to Prof. B. Visvanathan, IIT, Chennai for his suggestions in this work.

## References

[1] C.T. Kresge, M.E. Leonowicz, W.J. Roth, J.C. Vartuli, US Patent 5 098 684 (1992).
[2] C.T. Kresge, M.E. Leonowicz, W.J. Roth, J.C. Vartuli, J.S. Beck, Nature 359 (1992) 710.
[3] P.T. Tanev, M. Chibwe, T.J. Pinnavaia, Nature 368 (1994) 321.
[4] A. Corma, M.T. Navarro, J. Perez-Pariente, J. Chem. Soc., Chem. Commun. (1994) 147.
[5] K.M. Reddy, I. Moudrakovski, A. Sayari, J. Chem. Soc., Chem. Commun. (1995) 1059.
[6] J.S. Reddy, A. Sayari, J. Chem. Soc., Chem. Commun. (1995) 2231.
[7] T.K. Das, K. Chaudhari, A.J. Chandwadkar, S. Sivasanker, J. Chem. Soc., Chem. Commun. (1995) 2495.
[8] K. Chaudhari, T.K. Das, P.R. Rajmohan, K. Lazar, S. Sivasanker, A.J. Chandwadkar, J. Catal. 183 (1999) 281.
[9] N. Ulagappan, C.N.R. Rao, J. Chem. Soc., Chem. Commun. (1996) 1047.
[10] D.J. Jones, J. Jimenez-Jimenez, A. Jimenez-Lopez, P. Maireles-Torres, P. Rodriguez-Castellon, J. Roziere, J. Chem. Soc., Chem. Commun. (1997) 431.
[11] C.J.G. Van der Grift, A. Mulder, J.W. Geus, Appl. Catal. 60 (1990) 181.
[12] G.S. Jeon, J.S. Chung, Appl. Catal. A 115 (1994) 29.
[13] M. Arai, S. Nishiyama, S. Tsuruya, M. Masai, J. Chem. Soc., Faraday Trans. 92 (14) (1996) 2631.
[14] T. Komatsu, M. Nunokawa, I.S. Moon, T. Takahara, S. Namba, T. Yashima, J. Catal. 148 (1994) 427.
[15] S. Kieger, G. Delahay, B. Coq, B. Neveu, J. Catal. 183 (1999) 267.
[16] S. Kieger, G. Delahay, B. Coq, Appl. Catal. B 25 (2000) 1.
[17] S.W. Ham, H. Choi, I.S. Nam, Y.G. Kim, Catal. Lett. 42 (1996) 35.
[18] E.Y. Choi, I.S. Nam, Y.G. Kim, J. Catal. 161 (1996) 597.
[19] J. Okamura, S. Nishiyama, S. Tsuruya, M. Masai, J. Mol. Catal. A 135 (1998) 133.
[20] H. Fujiyama, I. Kohara, K. Iwai, S. Nishiyama, S. Tsuruya, M. Masai, J. Catal. 188 (1999) 417.
[21] D. Seebach, R. Dahinden, R.E. Marti, A.K. Beck, D.A. Plattner, F.N.M. Kuhnle, J. Org. Chem. 60 (1995) 1788.
[22] S. Kobayashi, H. Ishitani, J. Am. Chem. Soc. 116 (1994) 4083.
[23] M. Terada, Y. Motoyama, K. Mikami, Tetrahedron Lett. 35 (1994) 6693.
[24] E.M. Carreira, W. Lee, R.A. Singer, J. Am. Chem. Soc. 117 (1995) 3649.
[25] K. Maruoka, T. Itoh, T. Shirasaka, H. Yamamoto, J. Am. Chem. Soc. 110 (1988) 310.
[26] M. Shibasaki, H. Sasai, T. Arai, Angew. Chem. Int. Ed. Engl. 36 (1997) 1237.
[27] R. Noyori, I. Tomino, M. Nishizawa, J. Am. Chem. Soc. 106 (1984) 6709.
[28] M. Periasamy, J.V.B. Kanth, C.K. Reddy, J. Chem. Soc., Perkin Trans. I (1995) 427.
[29] F. Toda, K. Tanaka, S. Iwata, J. Org. Chem. 54 (1989) 3007.
[30] B. Feringa, H. Wynberg, J. Org. Chem. 46 (1981) 2547.

[31] K. Yamamoto, H. Fukushima, Y. Okamoto, K. Hatada, M. Nakazaki, J. Chem. Soc., Chem. Comm. (1984) 1111.
[32] B. Feringa, H. Wynberg, Tet. Lett. (1977) 4447.
[33] H.-K. Wang, J.-X. Xie, J.-J. Chang, K.-M. Hwang, S.-Y. Liu, L.M. Ballas, J.B. Jiang, K.-H. Lee, J. Med. Chem. 35 (15) (1992) 2717.
[34] A. Ortalm, J. Rathousky, G. Schulz-Ekloff, A. Zukal, Microporous Mater. 6 (1996) 171.
[35] X.S. Zhao, G.Q. Lu, J. Miller, J. Ind. Eng. Chem. Res. 35 (1996) 2075.
[36] M. Shimokawabe, N. Takazawa, H. Kobayashi, Bull. Chem. Soc. Jpn. 56 (1883) 1337.
[37] S.J. Gentry, N.W. Hurst, A. Jones, J. Chem. Soc. Faraday Trans. 173 (1979) 1688.
[38] A. Corma, V. Fornes, M.T. Navarro, J. Perez-Pariente, J. Catal. 148 (1994) 569.
[39] R. Mokaya, W. Jones, J. Chem. Soc., Chem. Commun. (1996) 983.
[40] A. Matsumoto, H. Chen, K. Tsutsumi, M. Grun, K. Unger, Microporous Mesoporous Mater. 32 (1999) 55.
[41] M.A. Kohler, H.E. Curry-Hyde, A.E. Hughes, B.A. Sexton, N.W. Cant, J. Catal. 108 (1987) 323.
[42] R.P. Eischens J. Jacknow, in: Proceedings of the Third International Congress on Catalysis 1964, North Holland, Amsterdam, 1965, p. 627.
[43] R. van Hardeveld, A. van Montfoort, Adv. Catal. 22 (1972) 75.
[44] V. Higgs, J. Pritchard, Appl. Catal. 25 (1986) 149.
[45] M. Shimokawabe, H. Asakawa, N. Takezawa, Appl. Catal. 59 (1990) 45.
[46] G. Centi, S. Perathoner, D. Biglino, E. Giamello, J. Catal. 151 (1995) 75.
[47] R.A. Schoonheydt, Catal. Rev.-Sci. Eng. 35 (1993) 129.
[48] M.C. Marison, E. Garbowski, M. Primet, J. Chem. Soc. Faraday Trans. 86 (1990) 3027.
[49] M. Shimokawabe, N. Takezawa, H. Kobayashi, Appl. Catal. 2 (1982) 379.
[50] J.S. Beck, J.C. Vartuli, W.J. Roth, M.W. Leonowicz, K.D. Schmit, C.T.-W. Chu, D.H. Olson, E.W. Sheppard, S.B. McCullen, J.B. Higgins, J.L. Schlenker, J. Am. Chem. Soc. 114 (1992) 10834.